Environmental Pollution 267 (2020) 115514

Contents lists available at ScienceDirect

Environmental Pollution

journal homepage: www.elsevier.com/locate/envpol

Estimating natural gas emissions from underground pipelines using surface concentration measurements☆☆

Younki Cho [a, *], Bridget A. Ulrich [b], Daniel J. Zimmerle [c], Kathleen M. Smits [a, d]

[a] Department of Civil Engineering, University of Texas Arlington, Arlington, TX, USA
[b] Natural Resources Research Institute, University of Minnesota Duluth, Duluth, MN, USA
[c] Energy Institute and Department of Mechanical Engineering, Colorado State University, Fort Collins, CO, USA
[d] Department of Civil and Environmental Engineering, Colorado School of Mines, Golden, CO, USA

ARTICLE INFO

Article history:
Received 15 June 2020
Received in revised form
18 August 2020
Accepted 24 August 2020
Available online 8 September 2020

Keywords:
Greenhouse gas
Methane
Fugitive emission
Distribution pipeline
Underground natural gas leakage
Pipeline safety

ABSTRACT

Rapid response to underground natural gas leaks could mitigate methane emissions and reduce risks to the environment, human health and safety. Identification of large, potentially hazardous leaks could have environmental and safety benefits, including improved prioritization of response efforts and enhanced understanding of relative climate impacts of emission point sources. However, quantitative estimation of underground leakage rates remains challenging, considering the complex nature of methane transport processes. We demonstrate a novel method for estimating underground leak rates based on controlled underground natural gas release experiments at the field scale. The proposed method is based on incorporation of easily measurable field parameters into a dimensionless concentration number, ε, which considers soil and fluid characteristics. A series of field experiments was conducted to evaluate the relationship between the underground leakage rate and surface methane concentration data over varying soil and pipeline conditions. Peak surface methane concentrations increased with leakage rate, while surface concentrations consistently decreased exponentially with distance from the source. Deviations between the estimated and actual leakage rates ranged from 9% to 33%. A numerical modeling study was carried out by the TOUGH3 simulator to further evaluate how leak rate and subsurface methane transport processes affect the resulting methane surface profile. These findings show that the proposed leak rate estimation method may be useful for prioritizing leak repair, and warrant broader field-scale method validation studies. A method was developed to estimate fugitive emission rates from underground natural gas pipeline leaks. The method could be applied across a range of soil and surface covering conditions.

1. Introduction

Natural gas has emerged as an attractive alternative to coal and oil because its combustion emits less carbon dioxide (CO_2) per unit energy, and it will likely remain a key heating fuel until more sustainable renewable fuels reach maturity. However, as methane (CH_4), the primary component of natural gas (NG), is a potent greenhouse gas (GHG, having a global warming potential of 86 times greater than CO_2 over a 20-year horizon) (IPCC, 2013), fugitive emissions from leaking NG pipelines have adverse environmental implications. Underground NG leaks are of particular concern, as they are not only difficult to detect and quantify, but also impose substantial safety concerns. Methane from underground NG leaks can accumulate in, and migrate through, subsurface environments and ultimately be released into the air or a substructure (Vetter et al., 2019), potentially causing explosions. Therefore, identification and repair of underground NG leaks is critical to protect public safety and the environment.

Several studies have sought to quantify anthropogenic methane emissions within local natural gas distribution pipelines (Gallagher et al., 2015; Jackson et al., 2014; Lamb et al., 2016; Phillips et al., 2013; von Fischer et al., 2017; Weller et al., 2018). For underground pipeline leak response efforts, bottom-up, local-level methods such as the surface enclosure and external tracer methods are commonly applied (Lamb et al., 2016; Weller et al., 2018; Zimmerle et al., 2017). The surface enclosure method estimates

☆ This paper has been recommended for acceptance by Prof. Pavlos Kassomenos.
* Corresponding author.
E-mail address: younki.cho@uta.edu (Y. Cho).

https://doi.org/10.1016/j.envpol.2020.115514
0269-7491/

underground leak rates by entraining underground gas in the air flow controlled by a Hi-Flow Sampler equipped with a surface enclosure, and then calculating leakage rate based on measured methane concentrations (Lamb et al., 2016, 2015; National Academies of Sciences, 2018; Weller et al., 2018). This method relies on the assumption that the leaking gas is captured, either by a single surface enclosure that is 1 m × 1 m in size (National Academies of Sciences, 2018) or a series of gridded enclosure placements to overcome the spatial limitation (Lamb et al., 2015). However, as previous results suggest that the methane expression area at the ground surface above an underground NG leak can extend across up to 6 m along the pipeline right-of-way for large leaks (Ulrich et al., 2019), it is possible that the surface enclosure method does not capture enough gas to support this assumption (Weller et al., 2018).

External tracer methods estimate methane leakage rates via release of a tracer gas at a known rate near the presumed source and measurement of downwind concentrations of tracer gas and methane. This method relies on two assumptions that could potentially be compromised due to inconsistent wind conditions: (i) complete mixing of methane and the tracer gas at the downwind measurement location, and (ii) highly similar co-dispersion of the tracer and target gas (methane) between source and measurement locations (Lamb et al., 1995; National Academies of Sciences, 2018; Roscioli et al., 2015; Shorter et al., 1997; Subramanian et al., 2015; Yacovitch et al., 2017). These methods require sophisticated implementation and measurement processes and advanced instrumentation that may not be readily available for routine field applications. On the other hand, taking advantage of existing resources such as walking survey data routinely collected by survey teams provides an efficient way to determine leakage rates. Though there has been less focus on the estimation of underground methane leakage rates using data collected during traditional walking surveys (e.g., surface concentration data), this information could be integral in prioritizing leak repair efforts.

Gas companies routinely perform walking surveys to inspect gas distribution pipelines and infrastructure for leaks, during which a portable, handheld methane detection device with parts-per-million level sensitivities is used to read surface methane concentrations (Weller et al., 2018). When a leak is located, surveyors approximate leak size and grade them from 1 to 3 based upon proximity to structures, rather than emission rate or leak size. This leak grading scheme is not applicable to estimation of GHG emissions from pipeline leaks. Simple and rapid methods to accurately quantify underground NG leak rates would thus enable better prioritization of underground NG leak response efforts. At a minimum, these methods should (i) be easily incorporated into common practices such as walking surveys, (ii) be based on readily measurable parameters, and (iii) have a verified accuracy. Controlled underground NG release experiments could enable both verification of estimation accuracy, as well as evaluation of relationships between leakage rate and parameters that are readily measurable during the walking surveys. Overall, bottom-up underground methane leakage rate estimation methods that account for methane transport in the shallow vadose zone could potentially lead to better understanding, quantifying, and tracking of emissions from individual emission sources.

We herein demonstrate a point-source bottom-up method to rapidly estimate underground NG leakage rates that is based on parameters that are readily measurable during walking surveys, and also incorporates an understanding of relevant subsurface methane transport processes. A dimensionless concentration number is proposed as a means of representing observed surface methane concentration distributions above an underground source, which considers fluid and physical system characteristics that control subsurface gas migration processes. Controlled underground NG release experiments were conducted at a field scale to verify the method and quantify its accuracy. To further evaluate how leak rate and subsurface methane transport processes affect the resulting methane surface profile, numerical modeling of methane transport in the shallow vadose zone and atmospheric domains was evaluated with a TOUGH3 simulator. The approach demonstrated herein could potentially enable rapid, evidence-based decision-making processes for leak repair prioritization efforts, allowing operators to more effectively target leaks that impose the greatest risk to the environment and public safety. These findings warrant broader field-scale method validation studies to assess the accuracy of the method over a wider range of conditions.

2. Materials and methods

Testbed configurations. Experiments were carried out at the Methane Emission Technology Evaluation Center (METEC), at Colorado State University in Fort Collins, CO, USA (Colorado State University, 2020). The site contains pipeline testbed sections that vary in configuration, allowing for simulation of underground NG pipeline leaks at known leakage rates. Subsurface conditions can be continuously monitored using soil moisture, temperature and pressure sensors installed in each testbed. The site also contains a meteorological station that measures windspeed, wind direction, barometric pressure, temperature, and humidity at 6 m above the ground. Wind speed and direction directly above the testbeds were also collected during each test using an ATMOS 22 portable ultrasonic anemometer and a ZL6 datalogger (METER Group, Inc.) recording at a 0.1 Hz frequency.

A generalized schematic depicting the underground testbeds is shown in Fig. 1A. Each testbed contains at least one underground 10 cm diameter polyvinylchloride (PVC) pipe (to simulate a realistic underground obstruction) running adjacent to stainless steel tubing which delivers the gas to underground controlled release points. Regulators, meters and valves control the natural gas release rate. The PVC pipes, while not filled with gas, provide subsurface conditions representative of a subsurface pipeline. Vapor implants (7.6 cm, Model 213860, Geoprobe, Salina, KS) at nearby underground locations enabled collection of subsurface gas samples and subsequent concentration measurement by gas chromatography mass spectrometry according to previously described methods (Ulrich et al., 2019) (see SI Appendix for details). Subsurface gas concentrations were used to calibrate the numerical model.

Two testbeds (Testbed A and B) were used in this study (Fig. 1B). Testbed A contains two pipelines: one pipeline with an adjacent stainless steel gas line (east−west, 0.91 m deep) and an additional pipeline without an adjacent gas line (northeast−southwest, 0.61 m deep). The additional intersecting pipeline simulates another co-located underground utility, as would be expected in a residential area. Testbed B contains only a single pipeline (east−west, 0.91 m deep), and is intended to simulate a rural area with no co-located or intersecting underground utilities. Excavations were backfilled with natural soil (soil texture classification: fine sand to loamy fine sand), such that the resulting permeability of the soil in the pipeline trenches is higher than that of the undisturbed soil (see prior publications (Mitton, 2018; Ulrich et al., 2019) for additional details). The coordinate system in Fig. 1 will be used for subsequent discussions. The origin [0 m, 0 m, 0 m] is located at the ground surface directly above the underground gas release point.

Experimental procedure. Surface measurements (i.e., measurements directly at the ground surface) were collected using a Gas-Rover (Bascom Turner Instruments VGI-201, CH_4 accuracy is greater of 20 ppm or 2% of reading at 1 Hz) equipped with a cone-

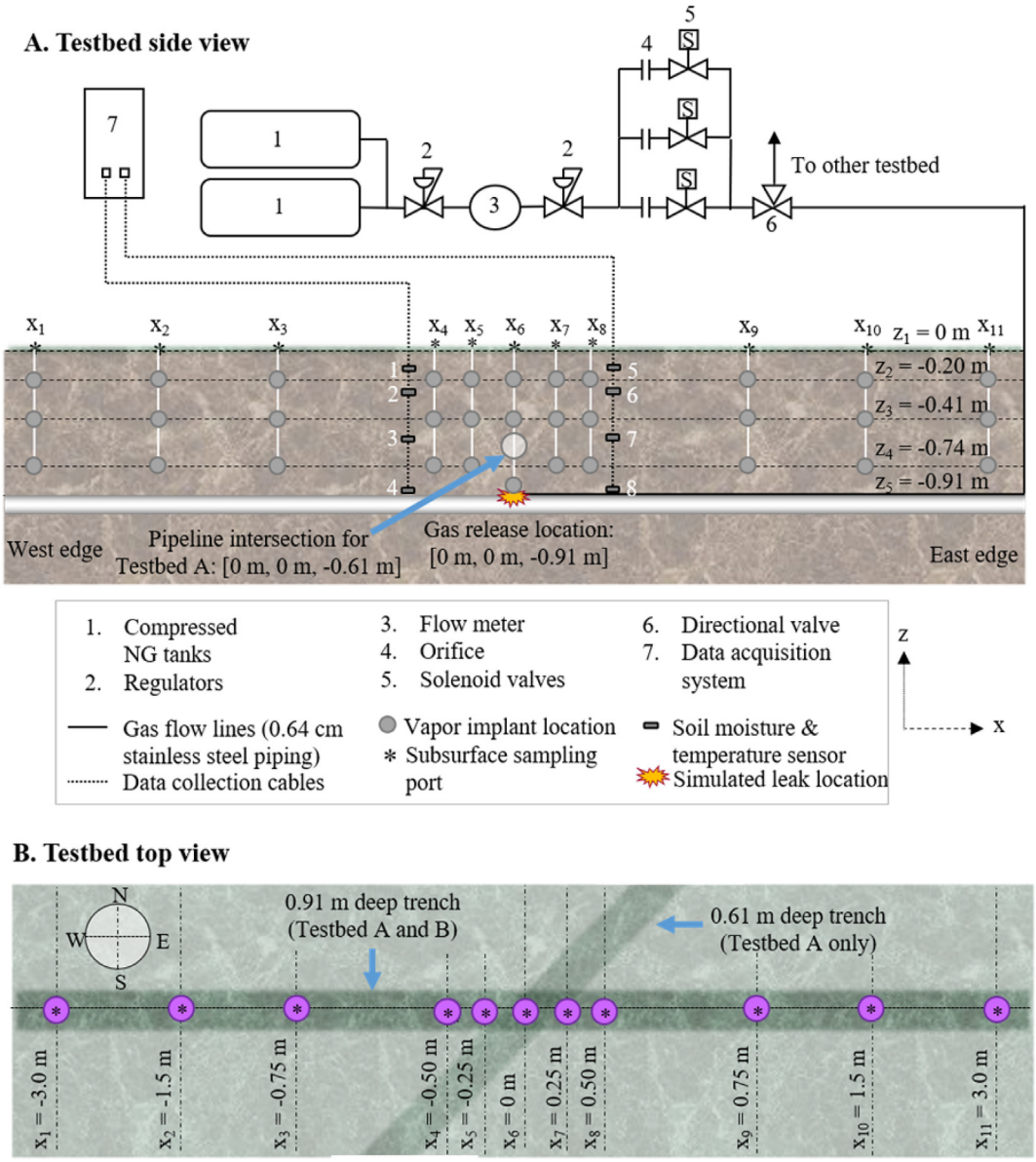

Fig. 1. Generalized schematics for underground testbeds (adapted from Ulrich et al. (2019)). (A) Generalized underground side view of testbeds indicating the location of the gas release, the pipelines, vapor implants, sampling ports, ancillary temperature and moisture sensors and associated data acquisition system, and gas flow control system. The white circle represents the position where the 0.61 m deep pipeline intersects the pictured trench cross section for Testbed A. Note that this intersecting pipeline is the only configurational difference between the testbeds. (B) Top view of the testbeds indicating the x-y locations for the pipeline trenches and the sampling ports.

shaped surface probe that enabled collection of surface flux data without wind interference. Surface measurements were collected over a 10 m × 8 m area of the testbed, centered above the leak location. The 10 m × 8 m area of the testbed was structured in a 15 × 9 grid. Surface CH_4 concentrations were measured at 135 grid points from north to south. As surface concentration measurements fluctuated over each measurement period with the Gas-Rover, surface methane measurements are reported as the maximum concentration observed over a 1–2 min measurement time.

A summary of the experimental and weather conditions for each experiment is shown in Table 1. Four steady state experiments were conducted with various flow rates (Exp. 1–4) while one transient experiment was carried out for numerical model calibration (Exp. 5). For steady state experiments, underground gas flow was initiated at least 12 h prior to measurement collection. Preliminary experiments indicated that gas reaches steady state in the testbed within approximately 8 h (Mitton, 2018). Depending on the experiment, flow rate (reported at kg/h of methane) was varied from 0.08 kg/h to 0.32 kg/h to represent a range of magnitudes for underground pipeline leaks. Though predicted leak rates based on above-ground concentration data from vehicle surveys are typically are less than 0.1 kg/h (Lamb et al., 2016; von Fischer et al., 2017; Weller et al., 2018; Zimmerle et al., 2017); the relatively large simulated leak rates from the present study are justified given our goal to prioritize large and potentially dangerous leaks. Previous results indicated that the diurnal changes in weather conditions experienced over the duration of each experiment (approximate 8 h) had little effect on the subsurface plume (Ulrich et al., 2019).

2.1. Numerical modeling

Simulations were performed using the multiphase flow

Table 1
Summary of experimental conditions. Flow rates are reported as kg/h of methane. The reference wind speed is the wind speed measured at 6 m height and averaged over the duration of the experiment. Error values for the wind speed and flow rate (standard deviations) are noted in parentheses.

Exp. #	Exp. Ref.	Testbed	Steady state/transient	Flow rate (kg/h)	Reference windspeed (m/s)
1	A-SS-0.08 kg/h	A	Steady state	0.08 (0.01)	2.6 (1.0)
2	A-SS-0.18 kg/h	A	Steady state	0.18 (0.01)	3.5 (1.2)
3	A-SS-0.27 kg/h	A	Steady state	0.27 (0.01)	2.3 (1.0)
4	B-SS-0.32 kg/h	B	Steady state	0.32 (0.01)	2.7 (1.0)
5	A-TR-0.19 kg/h	A	Transient	0.19 (0.01)	2.4 (1.6)

simulator, TOUGH3, combined with the equation of state module, EOS7CA to represent the CH_4 migration. TOUGH3/EOS7CA models Darcy flow and Fickian diffusive transport containing five components (water, brine, methane, air, and gas tracer) in gaseous and aqueous phases at near-ambient air pressures and temperatures (Oldenburg et al., 2010). The EOS7CA module was previously applied for modeling gas transport in the shallow subsurface (Lewicki et al., 2007; Oldenburg et al., 2010). Pressure and temperature dependent molecular diffusion coefficients are applied to model gas diffusion. In this work, diffusion is dominated by Brownian motion, and Knudsen diffusion is assumed to be negligible due to large pores in the soil. The thermodynamic properties of real gas mixtures are calculated by the Peng-Robinson equation of state. TOUGH3 calculates solubility of the gas components by Henry's law using methods outlined by Cramer (1982) to estimate Henry's law coefficients. Henry's law was applied to restrict the solubility of gaseous methane in the aqueous phase, and yields accurate predictions for pressures less than 1 MPa, as considered in this study (Oldenburg, 2015). The capillary pressure-saturation relationship and relative permeability are described using typical methods (Mualem, 1976; van Genuchten, 1980). A full description of the model equations can be found in Oldenburg (2015) and Jung et al. (2018).

Simulations were performed using a 3D computational domain, consisting of the porous subsurface system and an additional atmosphere system with discretized 89,600 grid blocks (Fig. 2). The subsurface domains were divided into two sections: disturbed and undisturbed soil, representing the excavated and backfilled pipeline region and undisturbed surrounding region, respectively. A horizontal well was installed in the disturbed soil section at a depth of approximately 1.0 m to represent the pipeline, and a dummy pipeline was treated as a fracture which was assigned at 0.61 m. A Dirichlet boundary condition (i.e. constant pressure) was imposed on the boundaries as shown in Fig. 2. In the atmospheric domain, a constant pressure was assigned between the upstream and downstream boundaries of the surface layer. All simulations were run under non-isothermal conditions. Prior to the simulation, steady-state gravity capillary equilibrium was reached by simulating the domain without gas release from the well.

The numerical model was calibrated according to the transient data for measured subsurface concentrations in Testbed A from Exp. 5. As the objective was to assess how leak rate and subsurface conditions affect the resulting methane concentration profile at the ground surface, the model was calibrated according to subsurface concentrations. Subsurface methane samples were collected at 0.41 m below ground (directly above the emission point) over 16 h, and the CH_4 concentration was measured by gas chromatography (GC). The soil properties (i.e., permeability and porosity) were adjusted to match experimental data (Exp. 5) although the properties within Testbed A were previously measured (Mitton, 2018).

3. Results and discussion

Surface methane distribution results. Surface concentration results are shown in Fig. 3 for Testbed A (Fig. 3A–C) and Testbed B (Fig. 3D). Surface concentrations were measured twice during Experiment 2 (Fig. 3B and S2), indicating a shift in wind speed during the experiment from 2.8 ± 1.3 m/s to 3.8 ± 0.9 m/s resulted in minimal changes to the surface concentration profile. The methane surface expression area increased for Testbed A as the leak rate was increased from 0.08 kg/h to 0.27 kg/h. As expected, methane migrated preferentially along the pipeline trench, likely due to the higher permeability of the trench soil versus the undisturbed soil. The oblong shape of the surface plume for the testbed B also reflected preferential migration along the pipeline trench. However, despite a slightly higher flow rate (Exp. 3 vs. Exp. 4), the plume for testbed B did not extend as far along the trench: the plume for testbed B extended approximately 4 m from the source, versus approximately 5 m for testbed A. This may have been caused by differences in the soil structure and pore geometry (permeability) of the trench and undisturbed soils between the two testbeds, suggesting that even small variations in the flow path due to soil heterogeneity can have significant effects on the macroscopic transport.

Dimensionless number development. The surface expression concentrations for Exp. 1, 2, and 3 are plotted with distance from

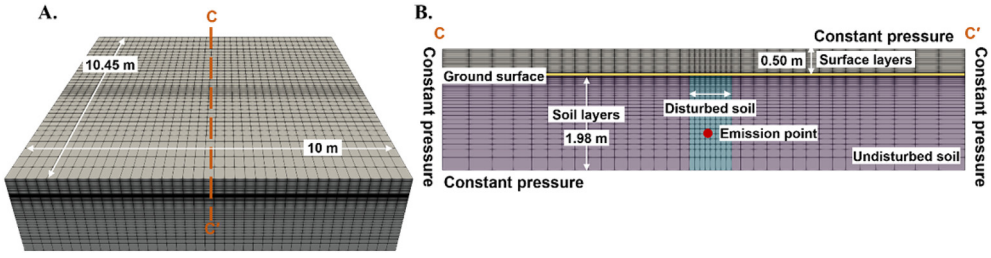

Fig. 2. (A) Domain discretization is illustrated and (B) the cross-sectional view of the brown dashed line CC′ in (A) is depicted. The boundary conditions are shown on all sides. The yellow line represents the ground surface. The red dot is an emission point at 1 m below the ground. The disturbed soil is shaded in blue while the undisturbed soil is in purple. The horizontal and vertical black lines represent the Cartesian grid. (For interpretation of the references to colour in this figure legend, the reader is referred to the Web version of this article.)

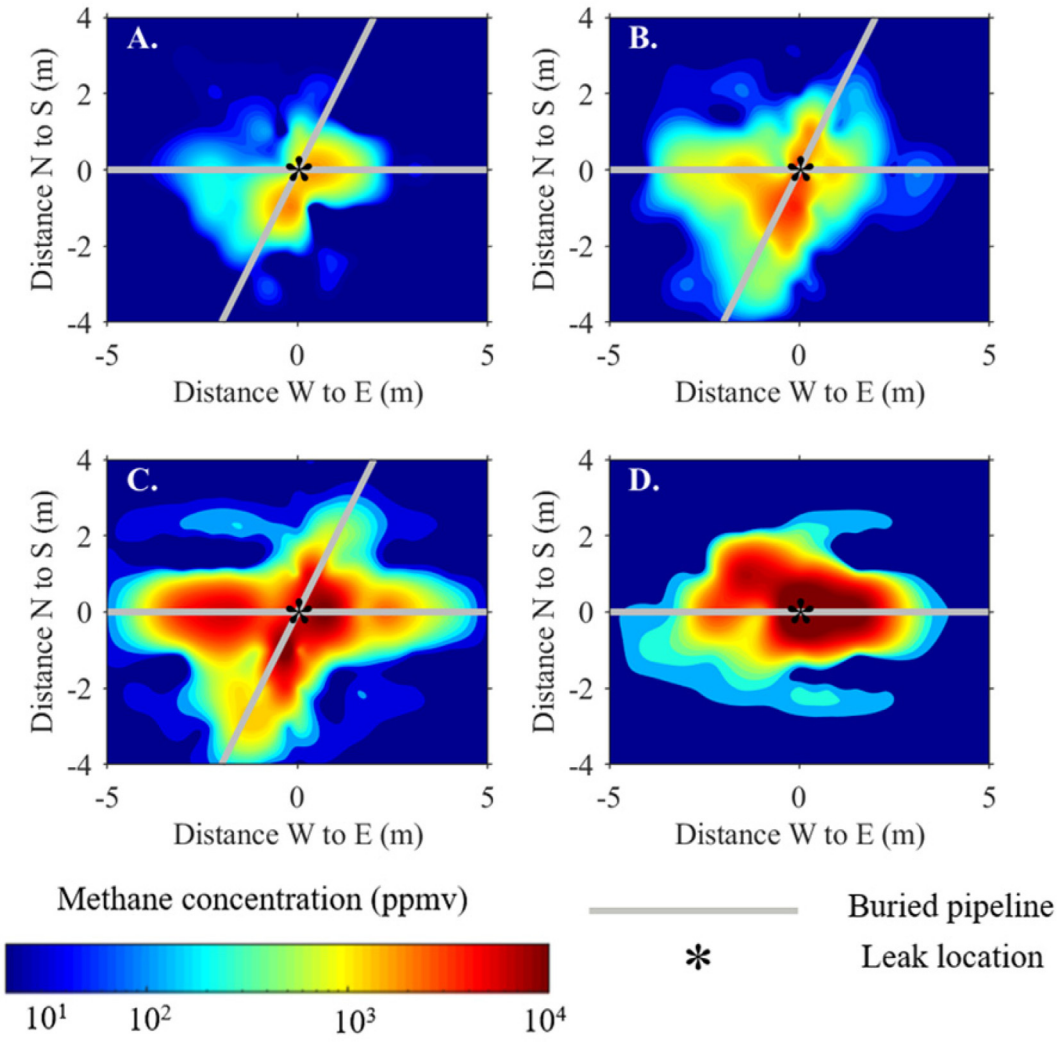

Fig. 3. (A–D) Steady state methane surface expression results for Exp. 1–4, respectively.

the emission source in Fig. 4A, revealing trends in the concentration profiles associated with increasing leak rate. Under the simple surface conditions evaluated herein (bare or poorly vegetated find sand soil without impermeable surface cover), concentrations decrease rapidly with distance from the source. At distances greater than 2.5 m, the surface concentration shows little dependence on leak rate relative to peak concentrations, while the surface concentration directly above the leak shows an approximately linear increase with leak rate (Fig. 4B). These observations suggest that it may be possible to generalize the surface concentration profile in a manner that is independent of leak rate.

A dimensionless term incorporating soil and fluid properties was derived to reflect subsurface conditions and the gas characteristics. Previous studies assessing methane transport in the shallow vadose zone have revealed that subsurface methane migration, driven primarily by advection and diffusion, is strongly affected by soil properties (e.g., permeability and moisture content) (Deepagoda et al., 2018; Felice et al., 2018; Mitton, 2018; Poulsen et al., 2001, 2003; Praagman and Rambags, 2008; van den Pol-van Dasselaar et al., 1998) and to a lesser extent by atmospheric properties (e.g., wind and changes in atmospheric pressure) (Deepagoda et al., 2018; Forde et al., 2019). This dimensionless concentration number, ε, is shown in equation (1):

$$\varepsilon = \frac{ckk_{rg}v_g z}{q\phi x b} \quad (1)$$

where c is methane concentration at the ground surface (mol/m^3), k is absolute permeability (m^2), k_{rg} is relative permeability of gas (fraction), ϕ is total porosity (fraction), v_g is the kinematic viscosity of methane (m^2/s), x is the distance from the leak source (m), b is the maximum length of methane extent at the ground surface (m), z is the depth to top of the leaking pipeline (m), and q is the methane leakage rate (mol/s). The average permeability of the soil in the testbed A was calculated from saturated hydraulic conductivity measured previously (Mitton, 2018). The porosity and water saturation were measured by a gravimetric method in the lab. The length of methane migration, b, is determined according to the location in the testbed where the surface concentration drops to a threshold level that is above background levels (here we use a threshold level of 300 ppm). The threshold level was determined based on the accuracy of the device used for surface measurements: the relative error of Gas-Rover (accuracy of greater of 20 ppm or 2% of reading) becomes less than 10% of the measurement when the concentration level is greater than or equal to 300 ppm. Thus, the threshold level was set to be at 300 ppm to

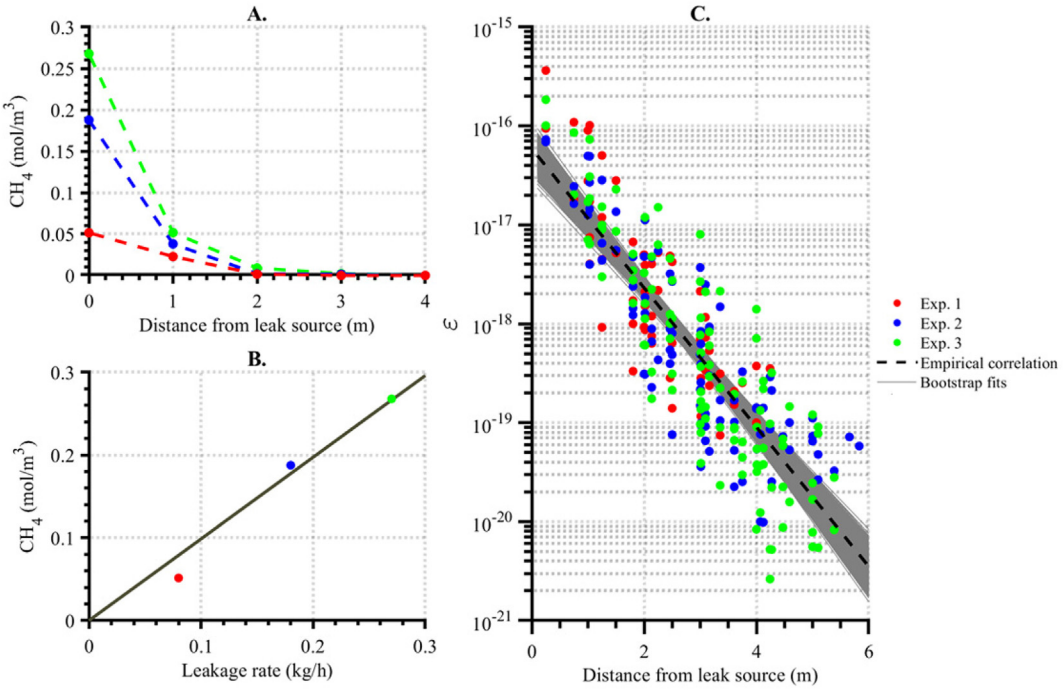

Fig. 4. (A) Representative one-dimensional concentration profiles of steady state methane surface expression results extracted from Exp. 1–3. (B) Surface concentration measured directly above the source versus leakage rate for the three profiles in panel A. The solid line is the linear trendline: $y = 0.99x$, $R^2 = 0.96$. (C) Dimensionless concentration number, ε, with the best-fit relation, Equation (2). The dashed black line represents the empirical correlation profile ($n = 261$, $R^2 = 0.27$).

minimize uncertainties in methane concentration. The depth of pipeline, z, is known, and constant throughout the testbed. This equation considers how methane surface concentration profiles are affected by soil and fluid properties that are either known, measurable, or can be estimated based on soil texture classification. A detailed description of the calculation of ε is shown in the SI.

We hypothesize that if ε is known for site-specific soil conditions, the leakage rate can be estimated based on the measured methane surface concentration profile (i.e., c vs. x). An empirical correlation of dimensionless concentration for specific soil texture can be derived from experiments, and then, the formulation of ε (Equation (1)) is rearranged to estimate leakage rate. It is important to emphasize that the methane concentration for ε is measured at the ground surface, and that ε will change depending on the soil conditions. The proposed dimensionless concentration number approach assumes (1) uniform soil properties throughout the testbed and (2) uniform distribution of water in soil. Different surface covers such as asphalt and concrete were not evaluated and may affect gas migration and surface readings. Further, for an actual underground NG leak, the distance between a measurement point and leak location cannot be known a priori. In this study, we assumed that the maximum surface concentration is located directly above the leak. While this may not be true for all cases, it is a suitable approximation if the goal of the method is to estimate leak size rather than leak location. The novelty of the approach is a simple, rapid estimate of underground NG leak rates using surface CH_4 concentrations measured regularly during walking surveys.

To derive an empirical correlation that could be used to demonstrate the dimensionless number leak rate estimation method, we used the best-fit exponential correlation of ε vs. x according to the surface concentration data from the controlled release experiments with varying leak rates (Exp. 1–3, testbed A). The parameters used to calculate ε are listed in Table 2. Equation (2) shows the resulting best-fit equation for the empirical correlation of ε as a function of distance from the center of the surface plume.

Table 2
Parameters for derivation of dimensionless concentration number, ε, from data from Exp. 1–3.

Parameter	Value
Total porosity[a], ϕ, fraction	0.45
Absolute permeability[b], k, m^2	2.18×10^{-13}
Water saturation[a], s_l, fraction	0.25
Relative permeability of gas[c] at $s_l = 0.25$, k_{rg}, fraction	0.61
Kinematic viscosity[d], ν_g, m^2/s	2.10×10^{-5}
Depth of leaking pipe, z, m	0.91
Leakage rate, q, kg/h	0.08 (Exp. 1)
	0.18 (Exp. 2)
	0.27 (Exp. 3)
Maximum migration distance, b, m	3.35 (Exp. 1)
	5.50 (Exp. 2)
	8.90 (Exp. 3)

[a] Measured by a gravimetric method.
[b] Estimated from saturated hydraulic conductivity (Mitton, 2018) assuming fluidity of 9.81×10^6 $m^{-1}s^{-1}$ at 20 °C.
[c] Corey (1954).
[d] Lemmon et al. (2005).

Fig. 4C shows that the correlation between the methane surface concentration profile is independent of leak rate for the tested conditions (0.08–0.27 kg/h).

$$E = Ae^{Bx} \quad (2)$$

where A and B coefficients with the 95% confidence interval (CI) in brackets are $A = 5.90 \times 10^{-17}[3.94 \times 10^{-17},\ 8.57 \times 10^{-17}]$ and $B = -1.62$ $[-1.75,\ -1.49]$, respectively. The confidence interval was determined by the bootstrap method.

The empirical correlation based on the data from testbed A (Exp. 1–3) was used to demonstrate the method for calculation of the leakage rate for Exp. 1–4. The rate was determined by the method of least squares, finding the best-fitting linear curve between $1/E$

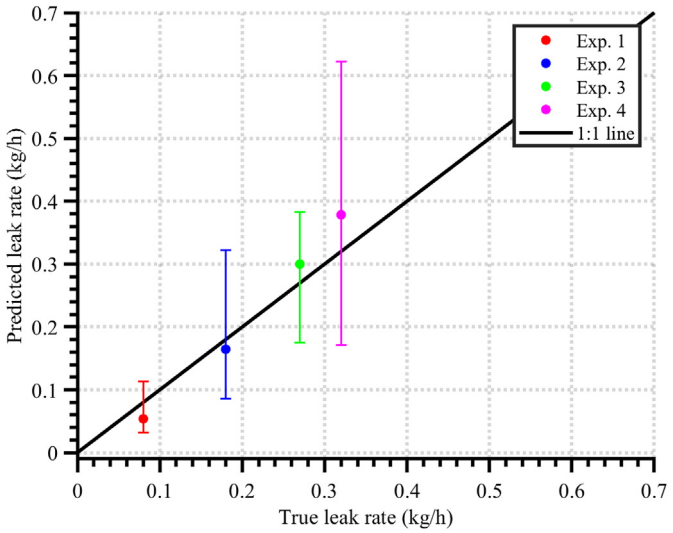

Fig. 5. A comparison of predicted vs. true leakage rates for controlled underground gas release experiments. The line is the 1:1 line. Error bars are 90% confidence interval calculated by the bootstrap method.

vs. $1/q\varepsilon$. The reciprocal of the best fit line slope represents the leakage rate (see SI Appendix for details). The data points (total of $n = 144$ points) measured within 2.5 m from the source were used to achieve the best results. The accuracy of the prediction is illustrated in Fig. 5A by comparison of the estimated rate to the 1:1 line. The 90% confidence interval calculated by the bootstrap method is shown in error bar. When the true and estimated rates are compared in a multiplicative relationship (i.e., $y = Ax$), the ratio yields 1.10 (95% CI = [0.88, 1.32], $n = 4$). The differences between true and estimate values range from 9% to 33% (average of 18%). A previous study found differences in the estimated rates between the surface enclosure and external tracer methods ranged from 5% to 50% (averaging 19%) over leak rates of 0.012–0.113 kg/h (Lamb et al., 2015). In another study comparing the surface enclosure and external tracer method, the estimated rate from the enclosure method was 0.029 kg/h lower than the external tracer method on average (Weller et al., 2018). Overall, these results indicate that the quantification of underground leak rate can be accurately estimated by the method proposed here.

Numerical model calibration. When injection of methane into the vadose zone was simulated for transient model calibration simulations, CH_4 began to fill the zone around the well and move upward. The maximum concentration was observed directly above the well because buoyancy and the pressure gradient drive methane to flow upward. Noticeable lateral movement occurred once the CH_4 reached pipeline trench at a depth of 0.61 m. The results of the numerical model calibration are presented in Fig. S1, and the resulting parameters (Table 3) were in a reasonable range of soil properties. The simulations were more sensitive to changes in the permeability than porosity. The permeabilities range from 8.00×10^{-14} m^2 to 4.21×10^{-13} m^2 with standard deviation of 1.80×10^{-13} m^2 (Mitton, 2018), and the fitted permeabilities were an order of magnitude lower. Previous studies have shown that permeability estimated from hydraulic conductivity for the same soil type of the testbed such as fine sand varies from 2.04×10^{-14} m^2 to 2.04×10^{-11} m^2 (Domenico and Schwartz, 1990) while loamy fine sand are from 2.83×10^{-15} m^2 to 5.35×10^{-11} m^2 (García-Gutiérrez et al., 2017). When the uncertainty in the permeability estimates are taken into consideration with respect to the wide range of permeability for the soil texture, the permeability used for calibration is justified. The discrepancy between the model and the calibration data was up to 24%, averaging 10% (Fig. S1). The experimental results reflect previous findings that subsurface methane concentrations can be greater than or equal to 80 vol% in the vicinity of the leak point after steady state is reached (Okamoto and Gomi, 2011). The calibrated model simulations resulted in an 8% higher steady state subsurface methane concentration than observed in the experiment. The remaining amount of air in the pore space at steady state for the experiment was 13%, which is considered high since air is a non-wetting phase that can be easily displaced by methane. Previous experimental and modeling results have shown that upward flow due to buoyancy and pressure-gradients forces methane to replace air in subsurface pore space (Spangler et al., 2010; West et al., 2015). This deviation could be caused by variability in soil conditions likely created by preferential flow paths for methane and left air trapped in pore, or by experimental error involved in sampling subsurface methane.

Numerical model simulations. Numerical simulations with the calibrated model were run to determine if simulated transport processes in the shallow vadose zone and the near-surface atmosphere reflect observed trends in the surface concentration profile. Simulations of methane injection from the horizontal well were run with the calibrated model over a range of rates, from 0.01 kg/h up to 0.3 kg/h, including the same rates as Exp. 1–3 (0.08, 0.18, and 0.27 kg/h) as well as two lower rates (0.01 and 0.05 kg/h).

The simulated surface expression profiles in general reflected the trends observed in the experiments (Fig. S6). As observed in experiments, the maximum surface concentration increases as the leak rate increases. While the simulation predicted the maximum surface concentrations to be directly above the leak source, the observed maximum surface concentrations were consistently located at [-0.25 m, -1 m], or SW of the leak location along the upper pipeline trench (running SW to NE). This suggests that variability in soil conditions created preferential flow paths, causing surface measurements to deviate from simulations. Further, the simulated methane surface expression area expanded

Table 3
Physical properties and transport parameters of the two porous media for the calibrated model.

	Disturbed soil	Undisturbed soil
Total porosity, ϕ	0.45	0.40
Absolute permeability, k	3.05×10^{-14} m^2	2.60×10^{-14} m^2
Initial gas saturation, S_g	0.80	0.80
Capillary pressure, p_c	van Genuchten[a,b] $\lambda = 0.75$, $S_{lr} = 0.050$, $\alpha = 5.50 \times 10^{-5}$ Pa^{-1}, $p_{max} = 1 \times 10^5$ Pa, $S_{ls} = 0.45$	van Genuchten[a,b] $\lambda = 0.75$, $S_{lr} = 0.050$, $\alpha = 5.50 \times 10^{-5}$ Pa^{-1}, $p_{max} = 1 \times 10^5$ Pa, $S_{ls} = 0.45$
Relative permeability, k_r	van Genuchten[a,b] $\lambda = 0.75$, $S_{lr} = 0.053$, $S_{ls} = 0.45$, $S_{gr} = 0.03$	van Genuchten[a,b] $\lambda = 0.75$, $S_{lr} = 0.053$, $S_{ls} = 0.45$, $S_{gr} = 0.03$
Temperature, T	30 °C	30 °C

[a] Pruess (2005).
[b] van Genuchten (1980); λ is m in van Genuchten (1980).

SW to NE along the upper pipeline trench as the leak rate was increased, which is expected given that there is a lower upward migration distance to reach the surface. These simulation results reflect the trends observed for Exp. 1 and 2 (Fig. 3A and B) with flow rates of 0.08 and 0.18, respectively. However, for the highest leak rate of 0.27 kg/h, the simulations show the surface expression area to continue to expand along the upper pipeline trench (Fig. S6F), while the experimental results show that the surface plume expanded N to S along the lower pipeline trench (Fig. 3C). Localized surface concentration maxima above the lower pipeline trench (at locations [0 m, 0.75 m] and [0 m, −1.5 m]) suggest that preferential flow paths developed above the lower pipeline at this high flow rate, causing lateral expansion of the surface expression layer along the lower pipeline trench. Overall, comparison of the simulations and experimental results show that model predictions reflect experimental results for experiments with leak rates from 0.01 to 0.3 kg/h.

The leak rate estimation method was further applied to calculate leak rates based on simulated surface methane concentration profiles to assess how preferential flow paths that may affect the leak rate calculation (Fig. S9). This analysis showed that the difference between the actual and predicted leak rates ranges from 5% to 58%, averaging 25%. This is because the gas escaping along preferential flow paths is not accounted for in the model. However, it is possible that the method can still be used for quantitative leak rate estimation up to a certain threshold leak rate, as that the majority of leaks in urban areas are less than 0.1 kg/h (Weller et al., 2018). Further, while quantitative calculations may be less certain at higher flow rates, surface profile characteristics may be used to make qualitative assessments of the relative size of large leaks, aiding in efforts to prioritize leak repairs.

4. Conclusions

Data and analysis presented here indicate that a well-characterized ε could provide a better analytic tool for estimating leak rate, using measurements that are readily performed during a leak survey. The basis of the method is the hypothesis that the methane surface expression area resulting from an underground leak is primarily controlled by transport processes in the subsurface. Comparisons of observed and simulated concentration profiles support this hypothesis, providing evidence that the method could be applied across a range of soil and surface covering conditions. As demonstrated by the work at METEC, future work is to further verify the method under a wider range of field conditions and run field measurements to the method on real leaks. Results from this study indicate that accuracies approaching those of current above-ground measurement methods may be achievable using substantially less labor-intensive approaches. This could enable broader adoption of leak size estimation into leak survey protocols, leading to concomitant improvements in both greenhouse gas emissions and safety classification.

Author contributions

Younki Cho: Conceptualization, Data curation, Methodology, Software, Formal analysis, Investigation, Writing—Original Draft, Writing—Review and Editing, Visualization. **Bridget A. Ulrich:** Methodology, Conceptualization, Investigation, Formal Analysis, Writing—Review and Editing. **Daniel J. Zimmerle:** Conceptualization, Methodology, Project Administration, Funding Acquisition, Writing—Review and Editing. **Kathleen M. Smits:** Conceptualization, Methodology, Investigation, Resources, Writing—Review and Editing, Supervision, Funding acquisition, Project administration.

Declaration of competing interest

The authors declare that they have no known competing financial interests or personal relationships that could have appeared to influence the work reported in this paper.

Acknowledgements

This material is based upon work supported by the Department of Energy (DOE) Advanced Research Projects Agency-Energy (ARPA-E) Methane Observation Networks with Innovative Technology to Obtain Reductions (MONITOR) program under Grant No. DE-FOA-0001546, the US Department of Transportation (DOT) Pipeline and Hazardous Materials Safety Administration (PHMSA) under Grant No. 693JK31810013 and the National Science Foundation Project Award Number 1447533. Any opinion, findings, and conclusions or recommendations expressed herein are those of the authors and do not necessarily reflect the views of those providing technical input or financial support. The trade names mentioned herein are merely for identification purposes and do not constitute endorsement by any entity involved in this study.

Appendix A. Supplementary data

Supplementary data to this article can be found online at https://doi.org/10.1016/j.envpol.2020.115514.

References

Colorado State University, 2020. Colorado state university energy institute METEC [CSU]. METEC. URL. https://energy.colostate.edu/metec/. (Accessed 27 May 2020).

Corey, A.T., 1954. The interrelation between gas and oil relative permeabilities. Prod. Mon. 19, 38–41.

Cramer, S.D., 1982. The Solubility of Methane, Carbon Dioxide, and Oxygen in Brines from 0 C to 300 C. US Department of the Interior, Bureau of Mines.

Deepagoda, C.T., Mitton, M., Smits, K., 2018. Effect of varying atmospheric conditions on methane boundary-layer development in a free flow domain interfaced with a porous media domain. Greenh. Gases 8, 335–348. https://doi.org/10.1002/ghg.1743.

Domenico, P.A., Schwartz, F.W., 1990. Physical and Chemical Hydrogeology. John Wiely and Sons. Inc., New York, New York.

Felice, M., de Sieyes, N., Peng, J., Schmidt, R., Buelow, M., Jourabchi, P., Scow, K., Mackay, D., 2018. Methane transport during a controlled release in the vadose zone. Vadose Zone J. 17, 1–11. https://doi.org/10.2136/vzj2018.02.0028.

Forde, O.N., Cahill, A.G., Beckie, R.D., Mayer, K.U., 2019. Barometric-pumping controls fugitive gas emissions from a vadose zone natural gas release. Sci. Rep. 9, 1–9. https://doi.org/10.1038/s41598-019-50426-3.

Gallagher, M.E., Down, A., Ackley, R.C., Zhao, K., Phillips, N., Jackson, R.B., 2015. Natural gas pipeline replacement programs reduce methane leaks and improve consumer safety. Environ. Sci. Technol. Lett. 2, 286–291. https://doi.org/10.1021/acs.estlett.5b00213.

García-Gutiérrez, C., Pachepsky, Y., Martín, M.Á., 2017. Saturated hydraulic conductivity and textural heterogeneity of soils. Hydrol. Earth Syst. Sci. 22, 3923–3932. https://doi.org/10.5194/hess-2017-706.

IPCC, 2013. Climate Change 2013: the Physical Science Basis: Working Group I Contribution to the Fifth Assessment Report of the Intergovernmental Panel on Climate Change. Cambridge University Press.

Jackson, R.B., Down, A., Phillips, N.G., Ackley, R.C., Cook, C.W., Plata, D.L., Zhao, K., 2014. Natural gas pipeline leaks across Washington, DC. Environ. Sci. Technol. 48, 2051–2058. https://doi.org/10.1021/es404474x.

Jung, Y., Pau, G.S.H., Finsterle, S., Doughty, C.A., 2018. TOUGH3 User's Guide, Version 1.0. Lawrence Berkeley National Lab. (LBNL), Berkeley, CA (United States). https://doi.org/10.2172/1461175.

Lamb, B.K., Cambaliza, M.O.L., Davis, K.J., Edburg, S.L., Ferrara, T.W., Floerchinger, C., Heimburger, A.M.F., Herndon, S., Lauvaux, T., Lavoie, T., Lyon, D.R., Miles, N., Prasad, K.R., Richardson, S., Roscioli, J.R., Salmon, O.E., Shepson, P.B., Stirm, B.H., Whetstone, J., 2016. Direct and indirect measurements and modeling of methane emissions in indianapolis, Indiana. Environ. Sci. Technol. 50, 8910–8917. https://doi.org/10.1021/acs.est.6b01198.

Lamb, B.K., Edburg, S.L., Ferrara, T.W., Howard, T., Harrison, M.R., Kolb, C.E., Townsend-Small, A., Dyck, W., Possolo, A., Whetstone, J.R., 2015. Direct measurements show decreasing methane emissions from natural gas local distribution systems in the United States. Environ. Sci. Technol. 49, 5161–5169. https://doi.org/10.1021/es505116p.

Lamb, B.K., McManus, J.B., Shorter, J.H., Kolb, C.E., Mosher, Byard, Harriss, R.C.,

Allwine, Eugene, Blaha, Denise, Howard, Touche, Guenther, Alex, Lott, R.A., Siverson, Robert, Westburg, Hal, Zimmerman, Pat, 1995. Development of atmospheric tracer methods to measure methane emissions from natural gas facilities and urban areas. Environ. Sci. Technol. 29, 1468–1479. https://doi.org/10.1021/es00006a007.

Lemmon, E.W., McLinden, M.O., Friend, D.G., 2005. Thermophysical Properties of Fluid Systems, NIST Chemistry Webbook. NIST standard reference database number 69. http://webbook.nist.gov.

Lewicki, J.L., Oldenburg, C.M., Dobeck, L., Spangler, L., 2007. Surface CO2 leakage during two shallow subsurface CO2 releases. Geophys. Res. Lett. 34 https://doi.org/10.1029/2007GL032047.

Mitton, M., 2018. Subsurface Methane Migration from Natural Gas Distribution Pipelines as Affected by Soil Heterogeneity: Field Scale Experimental and Numerical Study (Thesis). Colorado School of Mines. Arthur Lakes Library.

Mualem, Y., 1976. A new model for predicting the hydraulic conductivity of unsaturated porous media. Water Resour. Res. 12, 513–522. https://doi.org/10.1029/WR012i003p00513.

National Academies of Sciences, Engineering, and Medicine, 2018. Improving Characterization of Anthropogenic Methane Emissions in the United States. The National Academies Press, Washington, DC. https://doi.org/10.17226/24987.

Okamoto, H., Gomi, Y., 2011. Empirical research on diffusion behavior of leaked gas in the ground. J. Loss Prevent Proc. 24, 531–540. https://doi.org/10.1016/j.jlp.2011.01.007.

Oldenburg, C.M., 2015. EOS7CA Version 1.0: TOUGH2 Module for Gas Migration in Shallow Subsurface Porous Media Systems. Lawrence Berkeley National Lab.(LBNL), Berkeley, CA (United States).

Oldenburg, C.M., Lewicki, J.L., Dobeck, L., Spangler, L., 2010. Modeling gas transport in the shallow subsurface during the ZERT CO2 release test. Transport Porous Media 82, 77–92. https://doi.org/10.1007/s11242-009-9361-x.

Phillips, N.G., Ackley, R., Crosson, E.R., Down, A., Hutyra, L.R., Brondfield, M., Karr, J.D., Zhao, K., Jackson, R.B., 2013. Mapping urban pipeline leaks: methane leaks across Boston. Environ. Pollut. 173, 1–4. https://doi.org/10.1016/j.envpol.2012.11.003.

Poulsen, T.G., Christophersen, M., Moldrup, P., Kjeldsen, P., 2001. Modeling lateral gas transport in soil adjacent to old landfill. J. Environ. Eng. 127, 145–153. https://doi.org/10.1061/(ASCE)0733-9372(2001)127:2(145).

Poulsen, T.G., Christophersen, M., Moldrup, P., Kjeldsen, P., 2003. Relating landfill gas emissions to atmospheric pressure using numerical modelling and state-space analysis. Waste Manag. Res. 21, 356–366. https://doi.org/10.1177/0734242X0302100408.

Praagman, F., Rambags, F., 2008. Migration of natural gas through the shallow subsurface, pp. 1–96.

Pruess, K., 2005. ECO2N: a TOUGH2 fluid property module for mixtures of water, NaCl, and CO2. No. LBNL–57952, 877331). https://doi.org/10.2172/877331.

Roscioli, J.R., Yacovitch, T.I., Floerchinger, C., Mitchell, A.L., Tkacik, D.S., Subramanian, R., Martinez, D.M., Vaughn, T.L., Williams, L., Zimmerle, D., Robinson, A.L., Herndon, S.C., Marchese, A.J., 2015. Measurements of methane emissions from natural gas gathering facilities and processing plants: measurement methods. Atmos. Meas. Tech. Discuss. 8 https://doi.org/10.5194/amt-8-2017-2015.

Shorter, J.H., McManus, J.B., Kolb, C.E., Allwine, E.J., Lamb, B.K., Mosher, B.W., Harriss, R.C., Howard, T., Lott, R.A., 1997. Collection of leakage statistics in the natural gas system by tracer methods. Environ. Sci. Technol. 31 https://doi.org/10.1021/es9608095, 2012–2019.

Spangler, L.H., Dobeck, L.M., Repasky, K.S., Nehrir, A.R., Humphries, S.D., Barr, J.L., Keith, C.J., Shaw, J.A., Rouse, J.H., Cunningham, A.B., 2010. A shallow subsurface controlled release facility in Bozeman, Montana, USA, for testing near surface CO2 detection techniques and transport models. Environ. Earth Sci. 60, 227–239. https://doi.org/10.1007/s12665-009-0400-2.

Subramanian, R., Williams, L.L., Vaughn, T.L., Zimmerle, D., Roscioli, J.R., Herndon, S.C., Yacovitch, T.I., Floerchinger, C., Tkacik, D.S., Mitchell, A.L., Sullivan, M.R., Dallmann, T.R., Robinson, A.L., 2015. Methane emissions from natural gas compressor stations in the transmission and storage sector: measurements and comparisons with the EPA greenhouse gas reporting program protocol. Environ. Sci. Technol. 49, 3252–3261. https://doi.org/10.1021/es5060258.

Ulrich, B.A., Mitton, M., Lachenmeyer, E., Hecobian, A., Zimmerle, D., Smits, K.M., 2019. Natural gas emissions from underground pipelines and implications for leak detection. Environ. Sci. Technol. Lett. 6, 401–406. https://doi.org/10.1021/acs.estlett.9b00291.

van den Pol-van Dasselaar, A., van Beusichem, M.L., Oenema, O., 1998. Effects of soil moisture content and temperature on methane uptake by grasslands on sandy soils. Plant Soil 204, 213–222. https://doi.org/10.1023/A:1004371309361.

van Genuchten, M.T., 1980. A closed-form equation for predicting the hydraulic conductivity of unsaturated soils 1. Soil Sci. Soc. Am. J. 44, 892–898. https://doi.org/10.2136/sssaj1980.03615995004400050002x.

Vetter, C.P., Kuebel, L.A., Natarajan, D., Mentzer, R.A., 2019. Review of failure trends in the US natural gas pipeline industry: an in-depth analysis of transmission and distribution system incidents. J. Loss Prevent Proc. 60, 317–333. https://doi.org/10.1016/j.jlp.2019.04.014.

von Fischer, J.C., Cooley, D., Chamberlain, S., Gaylord, A., Griebenow, C.J., Hamburg, S.P., Salo, J., Schumacher, R., Theobald, D., Ham, J., 2017. Rapid, vehicle-based identification of location and magnitude of urban natural gas pipeline leaks. Environ. Sci. Technol. 51, 4091–4099. https://doi.org/10.1021/acs.est.6b06095.

Weller, Z.D., Roscioli, J.R., Daube, W.C., Lamb, B.K., Ferrara, T.W., Brewer, P.E., von Fischer, J.C., 2018. Vehicle-based methane surveys for finding natural gas leaks and estimating their size: validation and uncertainty. Environ. Sci. Technol. 52, 11922–11930. https://doi.org/10.1021/acs.est.8b03135.

West, J.M., Jones, D.G., Annunziatellis, A., Barlow, T.S., Beaubien, S.E., Bond, A., Breward, N., Coombs, P., de Angelis, D., Gardner, A., Gemeni, V., Graziani, S., Green, K.A., Gregory, S., Gwosdz, S., Hannis, S., Kirk, K., Koukouzas, N., Krüger, M., Libertini, S., Lister, T.R., Lombardi, S., Metcalfe, R., Pearce, J.M., Smith, K.L., Steven, M.D., Thatcher, K., Ziogou, F., 2015. Comparison of the impacts of elevated CO2 soil gas concentrations on selected European terrestrial environments. Int. J. Greenh. Gas Con. 42, 357–371. https://doi.org/10.1016/j.ijggc.2015.07.020.

Yacovitch, T.I., Daube, C., Vaughn, T.L., Bell, C.S., Roscioli, J.R., Knighton, W.B., Nelson, D.D., Zimmerle, D., Pétron, G., Herndon, S.C., 2017. Natural gas facility methane emissions: measurements by tracer flux ratio in two US natural gas producing basins. Elem. Sci. Anth. 5, 69. https://doi.org/10.1525/elementa.251.

Zimmerle, D.J., Pickering, C.K., Bell, C.S., Heath, G.A., Nummedal, D., Pétron, G., Vaughn, T.L., 2017. Gathering pipeline methane emissions in Fayetteville shale pipelines and scoping guidelines for future pipeline measurement campaigns. Elementa 5. https://doi.org/10.1525/elementa.258.